

Using the Haken–Strobl–Reineker Model to Determine the Temperature Dependence of the Diffusion Coefficient

Published as part of *Journal of Chemical Theory and Computation* virtual special issue “First-Principles Simulations of Molecular Optoelectronic Materials: Elementary Excitations and Spatiotemporal Dynamics”.

William Barford*



Cite This: *J. Chem. Theory Comput.* 2024, 20, 6510–6517



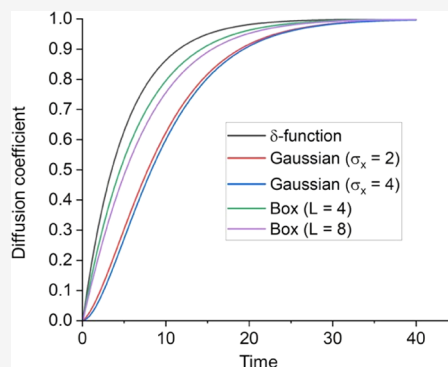
Read Online

ACCESS |

Metrics & More

Article Recommendations

ABSTRACT: Stochastic quantum Liouville equations (SQLE) are widely used to model energy and charge dynamics in molecular systems. The Haken–Strobl–Reineker (HSR) SQLE is a particular paradigm in which the dynamical noise that destroys quantum coherences arises from a white noise (i.e., constant-frequency) spectrum. A system subject to the HSR SQLE thus evolves to its “high-temperature” limit, whereby all the eigenstates are equally populated. This result would seem to imply that the predictions of the HSR model, e.g., the temperature dependence of the diffusion coefficient, have no validity for temperatures lower than the particle bandwidth. The purpose of this paper is to show that this assumption is incorrect for translationally invariant systems. In particular, provided that the diffusion coefficient is determined via the mean-squared-displacement, considerations about detailed-balance are irrelevant. Consequently, the high-temperature prediction for the temperature dependence of the diffusion coefficient may be extrapolated to lower temperatures, provided that the bath remains classical. Thus, for diagonal dynamical disorder the long-time diffusion coefficient, $D_{\infty}(T) = c_1/T$, while for both diagonal and off-diagonal disorder, $D_{\infty}(T) = c_1/T + c_2T$, where $c_2 \ll c_1$. An appendix discusses an alternative interpretation from the HSR model of the “quantum to classical” dynamics transition, whereby the dynamics is described as stochastically punctuated coherent motion.



1. INTRODUCTION

Coherent exciton dynamics in static, ordered molecular systems was described by Merrifield¹ in 1958. Assuming an exciton created at time $t = 0$ on a monomer, say $n = 0$, he showed that the subsequent wave function is $\Psi_n(t) = J_n(2\beta t)$, where J_n is the n th order Bessel function of the first-kind and β is the intermonomer exciton transfer integral. The wave function (illustrated in Appendix A) spreads ballistically with a constant speed and a mean-squared-displacement (MSD) increasing quadratically with time.

As Merrifield observed,¹ however, dynamics on a static, ordered system is an idealization. Various physical processes, e.g., exciton–phonon coupling, and static and dynamic disorder destroy the coherent motion, eventually causing incoherent (or diffusive) motion where the MSD increases linearly with time. This topic now has a long and rich history, with many reviews describing the state of the field.^{2–6}

The purpose of this paper is to expand on one particular rich area of investigation, namely the role of thermally induced noise in destroying quantum coherences. A notable paradigm in this subject is the so-called HSR stochastic quantum Liouville equation (SQLE), developed and investigated by Haken, Strobl and Reineker.^{2,7} This equation was developed from the

underlying time-dependent Schrödinger equation (TDSE) assuming that the dynamical fluctuations obey a white-noise spectrum, i.e., a constant power spectrum (or an Ohmic spectral function). Many important results have been derived from this model.^{2,8,9} In particular, it describes the “quantum to classical” transition, in which exciton dynamics exhibits a crossover from ballistic to diffusive behavior as a result of the noise destroying the coherent motion.

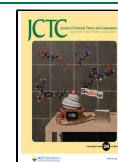
As stated, the HSR model assumes a white-noise spectrum, which implies that quantum transitions can occur between any pair of system energy eigenstates. This in turn implies that a system subject to the HSR SQLE evolves to its “high-temperature” limit, whereby all the eigenstates are equally populated. This result would seem to suggest that the predictions of the HSR model, e.g., the temperature dependence

Received: April 27, 2024

Revised: July 8, 2024

Accepted: July 8, 2024

Published: July 17, 2024



of the diffusion coefficient, have no validity for temperatures lower than the particle bandwidth. The purpose of this paper is to show that this assumption is incorrect for translationally invariant systems. In particular, provided that the diffusion coefficient is determined via the mean-squared-displacement, considerations about detailed-balance are irrelevant. Consequently, the high-temperature prediction for the temperature dependence of the diffusion coefficient may be extrapolated to lower temperatures, provided that the bath remains classical.

This key result will be proved in Section 2. Since the HSR SQLE predictions for the diffusion coefficient in translationally invariant systems are valid for temperatures lower than the particle bandwidth, the predictions of the underlying stochastic TDSE are also equally valid. We use this realization to reinterpret the quantum to classical transition as stochastically punctuated coherent motion. This is described in Appendix A.

Unlike the use of the MSD, Appendix B shows that the velocity autocorrelation function cannot be used to extrapolate the HSR predictions to temperatures lower than the bandwidth. Finally, Appendix C derives an expression for the temperature-dependence of the dephasing rate and Appendix D contains some details of the computational techniques.

2. THEORY

2.1. Model of Exciton Dynamics in Linear Molecular Systems. We formulate the problem in terms of Frenkel exciton dynamics in one-dimensional molecular systems, e.g., J-aggregates or conjugated polymers. However, the analysis applies equally to triplet excitons and charges.

The total Hamiltonian is

$$\hat{H} = \hat{H}_S + \hat{H}_{SB} + \hat{H}_B \quad (1)$$

where \hat{H}_S , \hat{H}_{SB} and \hat{H}_B are the system, system-bath and bath Hamiltonians, respectively. \hat{H}_B is defined in Appendix C (eq 47).

The system Hamiltonian is defined as

$$\hat{H}_S = \alpha \sum_{m=1}^N |m\rangle\langle m| + \beta \sum_{m=1}^N (|m+1\rangle\langle m| + |m\rangle\langle m+1|) \quad (2)$$

The ket $|m\rangle$ represents an exciton on monomer m , denoting a “site”, where N is the number of sites. α and β are the onsite potential and nearest-neighbor exciton transfer integral, respectively.

For a system with translational invariance, the eigenstates of \hat{H}_S are the Bloch states

$$|a\rangle = \frac{1}{\sqrt{N}} \sum_{m=1}^N \exp(ik_a m) \quad (3)$$

with eigenvalues $E_a = \alpha + 2\beta \cos k_a$, where $k_a = 2\pi a/N$ is the wavevector. The quantum numbers that label the eigenstates satisfy $1 \leq a \leq N$. The particle bandwidth in one-dimension is $4|\beta|$.

\hat{H}_{SB} is the system-bath Hamiltonian

$$\hat{H}_{SB} = \sum_m \delta\alpha_m(t) |m\rangle\langle m| + \sum_m \delta\beta_m(t) (|m+1\rangle\langle m| + |m\rangle\langle m+1|) \quad (4)$$

where $\delta\alpha_m(t)$ and $\delta\beta_m(t)$ represent dynamical fluctuations in α and β . These fluctuations are assumed to be uncorrelated in space, i.e.,

$$\langle \delta\alpha_m(t) \delta\alpha_n(0) \rangle = C_\alpha(t) = \sigma_\alpha^2 \exp(-t/\tau) \delta_{mn} \quad (5)$$

and

$$\langle \delta\beta_m(t) \delta\beta_n(0) \rangle = C_\beta(t) = \sigma_\beta^2 \exp(-t/\tau) \delta_{mn} \quad (6)$$

In addition, in the white noise limit, defined by $\sigma_x \tau \ll 1$, the bath correlation functions $C_x(t) \rightarrow 2\gamma_x \hbar^2 \delta(t)$, where $\gamma_x = \sigma_x^2 \tau / \hbar^2$ and \times indicates α or β . White noise means that the power spectrum, $I(\omega)$, is constant (or the spectral function, $J(\omega) \sim \omega I(\omega) \sim \omega$, i.e., Ohmic), which implies that the time-dependent part of the Hamiltonian induces transitions between all pairs of eigenstates.

For a classical, harmonic bath, $\gamma_x \propto \sigma_x^2 \propto k_B T$. More specifically, as shown in Appendix C, for linear system-bath coupling

$$\gamma_x = \pi k_B T E_x^r / \hbar^2 \omega_c \quad (7)$$

where E_x^r is the reorganization energy arising from the system-bath coupling and ω_c is a high-frequency cutoff for the spectral function.

2.2. Determining the Temperature-Dependent Diffusion Coefficient. The one-dimensional thermal diffusion coefficient as a function of time is defined as

$$\langle D(t, T) \rangle = \frac{1}{2} \frac{d}{dt} \text{Tr} \{ \hat{\rho}(t, T) \hat{x}^2(t) \} \quad (8)$$

where $\langle \dots \rangle$ indicates a thermal average, \hat{x} is the operator for the particle position, and $\hat{\rho}(t, T)$ is the system's reduced density operator. In the long-time limit the asymptotic diffusion coefficient is

$$\langle D_\infty(T) \rangle = \frac{1}{2} \frac{d}{dt} \text{Tr} \{ \hat{\rho}_0(T) \hat{x}^2(t) \} |_{\text{limit } t \rightarrow \infty} \quad (9)$$

where

$$\hat{\rho}_0(T) = \frac{\exp(-\hat{H}_S/k_B T)}{\text{Tr} \{ \exp(-\hat{H}_S/k_B T) \}} \quad (10)$$

is the equilibrium density operator.

Evaluating the trace over the eigenstate basis of \hat{H}_S , eq 9 becomes

$$\langle D_\infty(T) \rangle = \sum_a p_a(T) D_a \quad (11)$$

where

$$D_a = \frac{1}{2} \frac{d}{dt} \langle a | \hat{x}^2(t) | a \rangle |_{\text{limit } t \rightarrow \infty} \quad (12)$$

and $p_a(T)$ is the Boltzmann factor.

The mean-squared-displacement of a particle prepared in an arbitrary state $|\psi\rangle$ at $t = 0$ is defined as

$$\langle \psi | x^2(t) | \psi \rangle = \sum_m l^2 m^2 \rho_{mm}(t) \quad (13)$$

where l is the intermonomer separation and $\rho_{mm}(t)$ are the diagonal elements of the system density matrix in the site basis, $\{|m\rangle\}$. As described in Section 2.3, the density matrix, $\rho_{mn}(t)$, evolves according to an appropriate quantum Liouville equation with the initial condition $\rho_{mn}(0) = \langle m | \psi(0) \rangle \langle \psi(0) | n \rangle$.

Transforming to the eigenstate basis via a transformation matrix, S , eq 13 becomes

$$\langle \psi | x^2(t) | \psi \rangle = \sum_m l^2 m^2 \sum_{a,b} S_{ma} \tilde{\rho}_{ab}(t) S_{bm}^{-1} \quad (14)$$

where $\tilde{\rho}_{ab}$ is the density matrix in the eigenstate basis and $S_{ma} = \langle m|a \rangle$. For a system with translational invariance, the transformation matrix elements are the Bloch factors

$$S_{ma} = (S_{am}^{-1})^* = \frac{1}{\sqrt{N}} \exp(-ik_a m) \quad (15)$$

Splitting the double sum in eq 14 over a and b into the separate sums of $a = b$ and $a \neq b$, and using eq 15 we obtain

$$\langle x^2 \rangle = \frac{1}{N} \sum_m l^2 m^2 \left(1 + \sum_{a \neq b} \tilde{\rho}_{ab} \exp(i(k_b - k_a)m) \right) \quad (16)$$

where we have also used $\sum_a \tilde{\rho}_{aa} = 1$. The significance of this result is that it shows that for a translationally invariant system the diffusion coefficient of a particle prepared in the state $|\psi\rangle$ depends on the evolution of eigenstate coherences and not directly on the evolution of eigenstate populations. Moreover, as will be shown in Section 2.3, for a translationally invariant system, eigenstate coherences are decoupled from eigenstate populations, and thus for such systems the diffusion coefficient is completely independent of eigenstate populations. This means that when evaluating eq 11 to determine $\langle D_\infty(T) \rangle$ enforcing detailed balance—or ensuring that eigenstate populations satisfy their thermal values—is unnecessary. Thus, $\langle D_\infty(T) \rangle$ only depends on temperature parametrically via the temperature-dependence of the dephasing rate, eq 7.

Finally, as shown in Section 2.3, the asymptotic diffusion coefficient is independent of the initial state. Denoting this asymptotic value by $D_\infty(T)$, setting $D_a = D_\infty(T)$, $\forall a$, and using $\sum_a p_a = 1$, eq 11 becomes $\langle D_\infty(T) \rangle = D_\infty(T)$. Thus, our task now is to determine $D_\infty(T)$ for a given dephasing rate and for arbitrary initial conditions. This is achieved via the Haken–Strobl–Reineker model as described in the next section.

2.3. The Haken–Strobl–Reineker Model. Haken and Strobl showed that ensemble averages of observables determined via the stochastic TDSE may be evaluated by a SQLE.^{2,7} For the case of diagonal noise within the site basis, the SQLE reads

$$\frac{\partial \rho_{mn}}{\partial t} = -i(\beta/\hbar)(\rho_{m\pm 1,n} - \rho_{m,n\pm 1})\delta_{mn} - 2\gamma_\alpha \rho_{mn}(1 - \delta_{mn}) \quad (17)$$

Rotating to the eigenstate basis of \hat{H}_S via eq 15, the SQLE becomes for the populations

$$\frac{\partial \tilde{\rho}_{aa}}{\partial t} = -\sum_{b \neq a} (k_{ab}\tilde{\rho}_{aa} - k_{ba}\tilde{\rho}_{bb}) \quad (18)$$

and for the coherences

$$\frac{\partial \tilde{\rho}_{ab}}{\partial t} = -(i\omega_{ab} + 2\gamma_\alpha)\tilde{\rho}_{ab} + \frac{2\gamma_\alpha}{N} \sum_{c=1}^N \tilde{\rho}_{c,c+(b-a)} \quad (19)$$

where $\omega_{ab} = (E_a - E_b)/\hbar$.

From eqs 18 and 19 we note the following:

1. In the HSR model $k_{ab} = k_{ba} = 2\gamma_\alpha/N$, thus guaranteeing equal eigenstate populations in the long-time limit. In principle, one could impose detailed balance on the rates, thus ensuring that the populations equilibrate to their thermal values. However, as now shown, this is unnecessary.
2. The equations of motion for the populations and coherences are decoupled. This proves, by virtue of eq

16, that $\langle D_\infty(T) \rangle$ is independent of temperature-dependent populations and only depends on T parametrically via $\gamma_\alpha(T)$.

3. Equation 18 is a single N -coupled equation, whereas eq 19 are $(N-1) \times N$ -coupled equations. A numerical solution is described in Appendix D.

3. RESULTS

Haken, Reineker and co-workers derived an expression for $D(t)$ for an initial δ -function source.^{2,10} For diagonal noise this is

$$D(t) = \frac{\beta^2 l^2}{\hbar^2 \gamma_\alpha} (1 - \exp(-2\gamma_\alpha t)) \quad (20)$$

Reineker² also derived the asymptotic value, D_∞ , for arbitrary initial conditions. For diagonal noise

$$D_\infty = \beta^2 l^2 / \hbar^2 \gamma_\alpha \quad (21)$$

These analytical predictions were confirmed by solving both the HSR SQLE and the stochastic TDSE numerically (as described in Appendix D). Figure 1 shows the numerically

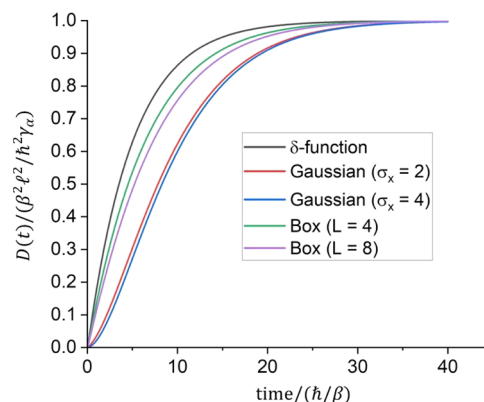


Figure 1. Computed $D(t)$ using eq 19 for various initial conditions and diagonal white noise, $\gamma_\alpha = 0.1\beta/\hbar$. For the δ -function source, $D(t)$ satisfies eq 20. The asymptotic values satisfy eq 21. The Gaussian wave functions are defined by eq 27. The particle-in-a-box wave functions are $\psi_n = (2/(L+1))^{1/2} \sin(\pi n/(L+1))$. The diffusion coefficient at short times for the Gaussian wave functions passes through a superlinear regime, as also reported in ref 11.

evaluated $D(t)$ for different initial conditions, namely a δ -function, Gaussian and particle-in-a-box sources. The δ -function result satisfies eq 20, while for all other sources, having a larger initial mean-squared-size and thus a smaller initial mean-squared-speed, the diffusion coefficient increases more slowly with time. However, eq 21 is satisfied for all initial conditions.

For translationally invariant systems, the evolution of the populations and coherences are also decoupled in the presence of off-diagonal noise. Thus, for both diagonal and off-diagonal noise, the high-temperature limit determined from the HSR SQLE can be extrapolated to temperatures lower than the bandwidth. Reineker² showed that for arbitrary initial conditions¹²

$$D_\infty = \frac{\beta^2 l^2}{\hbar^2 (\gamma_\alpha + 3\gamma_\beta)} + 2\gamma_\beta l^2 \quad (22)$$

where γ_α and γ_β are the diagonal and off-diagonal dephasing rates, respectively.

Substituting the temperature-dependence of the dephasing rates given by eq 7, we thus have the following prediction for the temperature-dependence of the diffusion coefficient in the presence of white noise:

$$D_{\infty}(T) = \frac{c_1}{T} + c_2 T \quad (23)$$

where

$$c_1 = \frac{\beta^2 \omega_c l^2}{\pi k_B (E_{\alpha}^r + 3E_{\beta}^r)} \quad (24)$$

and

$$c_2 = \frac{2\pi k_B E_{\beta}^r l^2}{\hbar^2 \omega_c} \quad (25)$$

Equation 23 is valid for translationally invariant systems subject to white noise for all temperatures—including temperatures lower than the particle bandwidth, $4|\beta|$ —provided that the bath remains classical. It remains valid if uniform long-range couplings are included, although the coefficients c_1 and c_2 are altered.

4. CONCLUSIONS

This paper has shown that for translationally invariant systems the predictions of the HSR model for the thermal diffusion coefficient can be extrapolated to temperatures lower than the particle bandwidth, provided that the bath remains classical. The proof relies on the observation that for such systems the mean-squared-displacement is independent of eigenstate populations. Consequently, considerations about detailed balance are irrelevant, and thus the diffusion coefficient depends on temperature only parametrically via the dephasing rates. When diagonal disorder dominates, $D(T) \sim T^{-1}$. This high-temperature limit for $D(T)$ is a common prediction in many theories of charge and energy transport.¹³

Translationally invariant systems subject to white noise are an idealization of more realistic systems, where static disorder, correlated (non-Markovian) noise and electron–phonon interactions causing polaron formation are all important processes that will modify the predictions of this paper. For such systems, numerical solutions of the TDSE or QLE should explicitly ensure that detailed balance and stationarity are maintained during the system's evolution (e.g., the Redfield quantum Liouville equation of motion,^{4,14–16} the time-dependent wavepacket diffusion method,^{17,18} hierarchical equations for open systems,¹⁹ and stochastic Liouville equation methods²⁰). The recently proposed MASH surface-hopping schemes^{21,22} are also promising techniques for such simulations.

We conclude by noting that in the presence of static, diagonal disorder the scaling of $D(T)$ with temperature deviates from the HSR prediction.^{8,9,23} In particular, for $\gamma \sim T < \beta$, $D(T) \propto T$. This increase of the diffusion coefficient with temperature at low temperatures, sometimes known as environment-assisted quantum transport,⁸ is a consequence of the thermal fluctuations destroying the Anderson localization arising from coherent superposition of the particle wave function.

■ APPENDIX A THE QUANTUM TO CLASSICAL TRANSITION

This appendix discusses an alternative interpretation from the HSR model of the “quantum to classical” dynamics transition,

whereby the dynamics is described as stochastically punctuated coherent motion.

In free space the one-dimensional TDSE reads

$$\frac{\partial \Psi(x, t)}{\partial t} = \frac{i\hbar}{2m} \frac{\partial^2 \Psi(x, t)}{\partial x^2} \quad (26)$$

where m is the particle mass. As is well-known,^{15,24} a particle prepared in a Gaussian wavepacket at $t = 0$, i.e.,

$$\Psi(x, 0) = \left(\frac{1}{2\pi\sigma_x^2(0)} \right)^{1/4} \exp(-x^2/4\sigma_x^2(0)) \quad (27)$$

undergoes a ballistic (or coherent) spread. Thus, its MSD, $\sigma_x^2(t)$, increases as

$$\sigma_x^2(t) = \sigma_x^2(0) + \frac{\hbar^2 t^2}{4m\sigma_x^2(0)} \quad (28)$$

In contrast, the diffusion equation describes the evolution of the density of an ensemble of particles, $\rho(x, t)$. In free space the one-dimensional diffusion equation reads

$$\frac{\partial \rho(x, t)}{\partial t} = D \frac{\partial^2 \rho(x, t)}{\partial x^2} \quad (29)$$

Although this equation has precisely the same mathematical form as eq 26, the absence of imaginary i means that its physical predictions are quite different. In particular, an initially localized distribution of particles spreads diffusively, i.e.,

$$\rho(x, t) = \left(\frac{1}{2\pi\sigma_x^2(t)} \right)^{1/2} \exp(-x^2/2\sigma_x^2(t)) \quad (30)$$

where the MSD increases as

$$\sigma_x^2(t) = \sigma_x^2(0) + 2Dt \quad (31)$$

The HSR equation describes how white noise causes a quantum particle's coherent motion to become incoherent. As shown by Reineker,² assuming a δ -function source on a lattice, i.e., $|\Psi_n(0)|^2 = \delta_{n0}$, for $t \ll 2\gamma$,

$$|\Psi_n(t)|^2 = J_n^2(2\beta t) \quad (32)$$

(as predicted by the TDSE on a lattice¹) where J_n is the n th-order Bessel function of the first kind. In contrast, for $t \gg 2\gamma$,

$$|\Psi_n(t)|^2 = \left(\frac{1}{4\pi Dt} \right)^{1/2} \exp(-n^2/4Dt) \quad (33)$$

(as predicted by the diffusion equation) where $D = \sigma_x^2(t)/2t = \beta^2/\gamma_{\alpha}$ for diagonal noise. In general for a δ -function source (where henceforth in this Appendix, we set $\hbar = l = 1$)^{2,25}

$$\sigma_x^2(t) = \frac{2\beta^2 t}{\gamma_{\alpha}} + \frac{\beta^2 t}{\gamma_{\alpha}^2} (\exp(-2\gamma_{\alpha} t) - 1) \quad (34)$$

In this interpretation, noise causes a crossover from coherent to incoherent motion. A different interpretation of the quantum to classical transition, however, is afforded by the Lindblad formulation of the quantum Liouville equation. As we now show, in this interpretation the particle's dynamics can be viewed as stochastically punctuated coherent motion.

1. The Lindblad dissipator is¹⁶

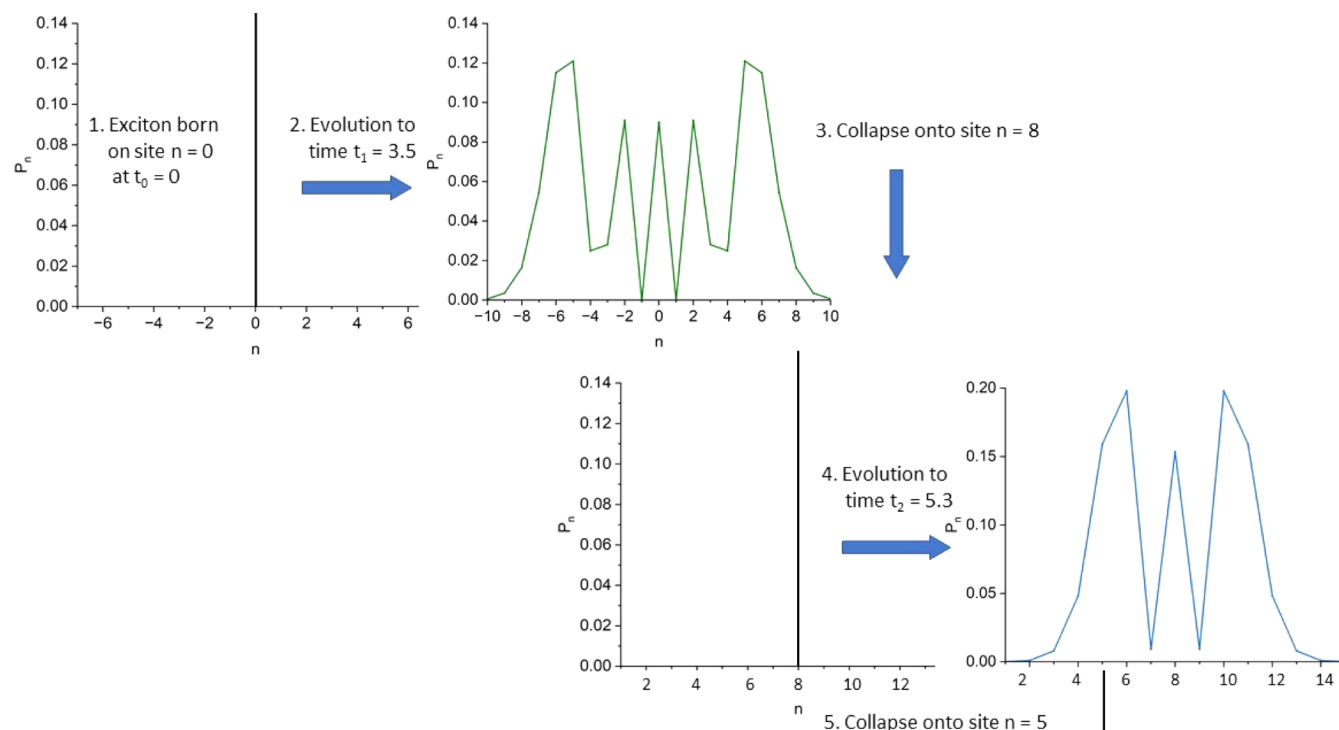


Figure 2. An illustration of the evolution of a particle wave function subject to the TDSE with stochastic wave function collapses caused by white noise. The particle probability, $P_n(t) = J_n^2(2\beta t)$. The cumulative effect of the stochastic wave function collapses is to cause particle diffusion, where $D = \beta^2/\gamma_\alpha$ in exact agreement with the HSR model. $\gamma_\alpha = 0.1\beta/\hbar$. Time is in units of \hbar/β .

$$\hat{L}[\hat{\rho}(t)] = \Gamma \sum_m \left(\hat{A}_m \hat{\rho}(t) \hat{A}_m^\dagger - \frac{1}{2} (\hat{A}_m^\dagger \hat{A}_m \hat{\rho}(t) + \hat{\rho}(t) \hat{A}_m^\dagger \hat{A}_m) \right) \quad (35)$$

where \hat{A}_m is the Lindblad jump operator. For diagonal white-noise,⁸ $\hat{A}_m = |m\rangle\langle m|$ and $\Gamma = 2\gamma_\alpha$.

2. An ensemble of quantum trajectories reproduces the observables obtained via a QLE if each trajectory undergoes nonunitary evolution via an effective non-hermitian Hamiltonian,²⁶ defined by

$$\begin{aligned} \hat{H}_S \rightarrow \hat{H}_{\text{eff}} &= \hat{H}_S - \frac{i\Gamma}{2} \sum_m \hat{A}_m^\dagger \hat{A}_m \\ &= \hat{H}_S - \frac{i\Gamma}{2} \sum_m |m\rangle\langle m| \end{aligned} \quad (36)$$

3. The simulation of a quantum trajectory then proceeds as follows:

- (a) Given $|\Psi(t)\rangle$ at a time t , compute

$$|\Psi_{\text{trial}}\rangle = \exp(-i\hat{H}_{\text{eff}}\delta t)|\Psi(t)\rangle \quad (37)$$

where δt is the time step. (See Appendix D for details.)

- (b) Determine δp , defined via $\langle \Psi_{\text{trial}} | \Psi_{\text{trial}} \rangle = 1 - \delta p$.

- (c) Then,

- (i) with a probability $(1 - \delta p)$ define

$$|\Psi(t + \delta t)\rangle = |\Psi_{\text{trial}}\rangle / (1 - \delta p)^{1/2} \quad (38)$$

In this case the wave function evolves according to \hat{H}_{eff} .

Or,

- (ii) with a probability δp define

$$|\Psi(t + \delta t)\rangle = \frac{\hat{A}_m |\Psi(t)\rangle}{\langle \Psi(t) | \hat{A}_m^\dagger \hat{A}_m | \Psi(t) \rangle^{1/2}} \quad (39)$$

Using the definition that $\hat{A}_m = |m\rangle\langle m|$, eq 39

implies that $|\Psi(t + \delta t)\rangle = |m\rangle$. Thus, in this case, the wave function collapses onto site m .

- (d) If a quantum jump occurs in 3(c)(ii), the site m is chosen with a probability $P_m = |\Psi_m(t)|^2$.

Thus, the effect of the Lindblad jump operator in step 3(c)(ii) is to collapse the coherently evolving wave function onto the site m , after which it then again expands coherently until the next collapse. This process is illustrated in Figure 2: At time $t = 0$ the particle is created on site $n_0 = 0$. Its wave function then evolves coherently until the first quantum jump at $t = t_1$. For $t \leq t_1$, $\Psi_n(t) = J_n(2\beta t)$, where J_n is the n th order Bessel function.¹ At $t = t_1$ the wave function collapses onto site $n = n_1$, whereupon it again evolves coherently until a time t_2 , when it again collapses onto site $n = n_2$.

As these collapses are stochastic in space and time, their cumulative effect is to cause particle diffusion. We can determine the diffusion coefficient as follows. For a diffusive process the MSD is defined as

$$\text{MSD}(t) = \sigma_x^2(t) = N(t)\langle l^2 \rangle \quad (40)$$

where $N(t) = t/\langle \tau \rangle$ is the number of jumps in a time t and $\langle \tau \rangle = 1/\Gamma = 1/2\gamma_\alpha$ is the average time interval between jumps. $\langle l^2 \rangle$ is the mean-squared jump size, determined by $\langle l^2 \rangle = \langle v^2 \tau^2 \rangle = v^2 \langle \tau^2 \rangle$, where v is the particle's coherent speed. For a δ -function source on a lattice, $v = \sqrt{2\beta}$. As

determined by simulating the TDSE with Lindblad jump operators, for the dynamics described here, $\langle \tau^2 \rangle = 2\langle \tau \rangle^2 = 2/(2\gamma_\alpha)^2$. Hence, $\langle l^2 \rangle = \beta^2/\gamma_\alpha^2$ and therefore $D = N(t)\langle l^2 \rangle/2t = \beta^2/\gamma_\alpha$, thus—on average—rederiving the prediction of the HSR quantum Liouville equation. Ensemble averaging over many particle trajectories will give precisely the same observables (e.g., average particle density) as the stochastic quantum Liouville approach, but the interpretation of the dynamics is different, namely stochastically punctuated coherent dynamics.

■ APPENDIX B USING THE VELOCITY AUTOCORRELATION FUNCTION

An alternative definition to the thermal diffusion coefficient from eq 8 is

$$\langle D(t, T) \rangle = \int_0^t \text{Tr} \{ \hat{\rho}(t', T) \hat{C}_v(t') \} dt' \quad (41)$$

where $\hat{C}_v(t) = \hat{v}(t)\hat{v}(0)$ is the velocity autocorrelation operator. The derivation of eq 41 from the identity

$$x^2(t) = \int_0^t \int_0^t v(t')v(t'')dt'dt'' \quad (42)$$

assumes stationarity, i.e., that the time-average of $v(t+t')v(t')$ is independent of t' .

However, if $\langle \psi | \hat{C}_v(t) | \psi \rangle$ is evaluated for an arbitrary state $|\psi\rangle$ via the HSR SQLE the stationarity condition is not met. This is because, unlike the case for the mean-squared-displacement, $\langle \psi | \hat{C}_v(t) | \psi \rangle$ depends on eigenstate populations, which become equally populated under evolution via the HSR SQLE.

Indeed, as shown in Figure 3,

$$C(t) = \langle \psi | \hat{C}_v(t) | \psi \rangle = \langle \psi | \hat{C}_v(0) | \psi \rangle \exp(-2\gamma_\alpha t) \quad (43)$$

in agreement with the definition^{9,14}

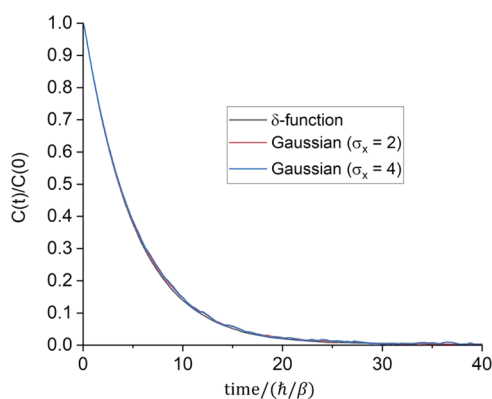


Figure 3. Velocity autocorrelation function, $C(t) = \langle \psi | \hat{C}_v(t) | \psi \rangle$, where $\hat{C}_v(t) = \hat{v}(t)\hat{v}(0)$, computed via the stochastic TDSE with diagonal white noise ($\gamma_\alpha = 0.1\beta/\hbar$). $C(t)$ satisfies eq 43 for any initial condition. $C(0) = \langle \hat{v} \rangle_0$ is $2\beta^2 l^2/\hbar^2$ for a δ -function, while it is $\beta^2/\hbar^2 \sigma_x^2$ for a Gaussian wavepacket (defined in eq 27), with σ_x in units of l and \hat{v} is defined in eq 60.

$$\hat{v}(t) = \exp(i\hat{H}t/\hbar)\hat{v}\exp(-i\hat{H}t/\hbar)\exp(-2\gamma_\alpha t) \quad (44)$$

for the HSR model. Integrating eq 43 over time gives

$$D_\infty = \frac{\langle \psi | \hat{C}_v(0) | \psi \rangle}{2\gamma_\alpha} \quad (45)$$

which erroneously predicts that the asymptotic diffusion coefficient depends on the initial condition.

Equation 45 is only correct for a δ -function source, because this maximally localized in real-space wave function is maximally delocalized in momentum-space, i.e., all the energy (momentum) eigenstates of a translationally invariant system are already equally populated at $t = 0$ so that the stationarity condition is automatically satisfied. Otherwise, for arbitrary initial conditions, eq 41 is only valid provided detailed balance is enforced. Such a scenario is described in ref 14.

■ APPENDIX C THE DEPHASING RATE

This appendix describes a derivation of eq 7.

For linear system-bath coupling, the system-bath Hamiltonian is¹⁵

$$\begin{aligned} \hat{H}_{\text{SB}} = & \sum_m |m\rangle\langle m| \sum_j c_{jm}^\alpha u_j + \sum_m (|m\rangle\langle m+1| \\ & + |m+1\rangle\langle m|) \sum_j c_{jm}^\beta u_j \end{aligned} \quad (46)$$

while the bath Hamiltonian of harmonic oscillators is¹⁵

$$\hat{H}_B = \frac{1}{2} \sum_j (\dot{u}_j^2 + \omega_j^2 u_j^2). \quad (47)$$

u_j are the mass-weighted oscillator displacements and c_j^\times are the weightings of each normal mode with associated spectral functions,

$$J_\alpha(\omega) = \frac{\pi}{2} \sum_j \frac{(c_j^\alpha)^2}{\omega_j} \delta(\omega - \omega_j) \quad (48)$$

The bath autocorrelation function associated with diagonal noise is $C_\alpha(t) = \langle \delta\alpha(t)\delta\alpha(0) \rangle$, where $\delta\alpha(t) = \sum_j c_j^\alpha u_j(t)$ is the dynamical fluctuation of the on-site potential energy. For a classical, harmonic bath and linear system-bath coupling¹⁵

$$C_\alpha(t) = \frac{2k_B T}{\pi} \int_0^\infty d\omega \frac{J_\alpha(\omega)}{\omega} \cos \omega t \quad (49)$$

The spectral function, $J_\alpha(\omega)$, for an Ohmic bath with a high-frequency cutoff, ω_c is defined as

$$J_\alpha(\omega) = \left(\frac{\pi E_\alpha^r \omega}{\omega_c} \right) \exp(-\omega/\omega_c) \quad (50)$$

E_α^r is the reorganization energy of the bath modes, satisfying

$$E_\alpha^r = \frac{1}{\pi} \int_0^\infty d\omega \frac{J_\alpha(\omega)}{\omega} \quad (51)$$

Thus, using

$$\int_0^\infty d\omega \exp(-\omega/\omega_c) \cos \omega t = \frac{\omega_c}{1 + (\omega_c t)^2} \rightarrow \pi \delta(t) \quad (52)$$

as $\omega_c \rightarrow \infty$, we obtain

$$C_\alpha(t) = \left(\frac{2\pi k_B T E_\alpha^r}{\omega_c} \right) \delta(t) \quad (53)$$

Equating eq 53 with the definition of γ_α given in Section 2.1, i.e., $C_\alpha(t) = 2\gamma_\alpha \hbar^2 \delta(t)$, yields an expression for the dephasing rate which is linearly proportional to temperature:

$$\gamma_\alpha = \frac{\pi k_B T E_\alpha^r}{\hbar^2 \omega_c} \quad (54)$$

■ APPENDIX D COMPUTATIONAL METHODS

D.1. Numerical Solution of the HSR Stochastic Quantum Liouville Equation

Since the equation of motion for the coherences in the eigenstate basis, eq 19, are block diagonal with respect to the quantum number c , there are $(N - 1) \times N$ -coupled equations. These can be cast into the general form

$$\frac{dP_i}{dt} = \sum_{j=1}^N L_{ij} P_j \quad (55)$$

for $1 \leq i \leq (N - 1)$, where L is the coupling matrix. The solution from linear algebra is

$$P_i(t) = \sum_{jk} S_{ij} \exp(\lambda_j t) S_{jk}^{-1} P_k(0) \quad (56)$$

where S is the matrix whose columns are the eigenvectors of L , $\{\lambda\}$ are the corresponding eigenvalues and $P_k(0)$ is an initial condition. To produce the results illustrated in Figure 1, the complex matrix L was diagonalized via the LAPACK routine ZGEEV, and the complex matrix S was inverted via the LAPACK routines ZGETRF and ZGETRI.

D.2. Numerical Solution of the Time-Dependent Schrödinger Equation

In general, given $\Psi(t)$ we require

$$\Psi(t + \delta t) = \exp(-i(H_S + H_{SB}(t))\delta t/\hbar)\Psi(t) \quad (57)$$

This is easily accomplished via the short iterative Lanczos propagator method,²⁴ whereby a Krylov space of N vectors is generated via the Lanczos method. Diagonalizing the tridiagonal Hamiltonian, H_{Lanczos} , within the Krylov space yields

$$\Psi(t + \delta t) = S \cdot \exp(-iD\delta t/\hbar) \cdot S^\dagger \Psi(t) \quad (58)$$

where S is the matrix whose columns are the eigenvectors of H_{Lanczos} , the diagonal elements of D are its eigenvalues, and $\Psi(t)$ is the first vector in the Krylov space.

The expectation value of the velocity autocorrelation function is

$$\begin{aligned} \langle \Psi | \hat{C}_v(t) | \Psi \rangle &= \langle \Psi | \hat{v}(t) \hat{v}(0) | \Psi \rangle \\ &= \langle \Psi(t) | \hat{v} | \Phi(t) \rangle \end{aligned} \quad (59)$$

where $|\Phi\rangle = \hat{v}|\Psi\rangle$ and the velocity operator on a lattice is

$$\hat{v} = i(l\beta/\hbar) \sum_m \langle lm | \langle m + 1 | - | m + 1 \rangle \langle ml | \rangle \quad (60)$$

■ AUTHOR INFORMATION

Corresponding Author

William Barford – Department of Chemistry, Physical and Theoretical Chemistry Laboratory, University of Oxford, Oxford OX1 3QZ, U.K.; orcid.org/0000-0002-7223-686X; Email: william.barford@chem.ox.ac.uk

Complete contact information is available at:

<https://pubs.acs.org/10.1021/acs.jctc.4c00568>

Notes

The author declares no competing financial interest.

■ REFERENCES

- (1) Merrifield, R. E. Propagation of Electronic Excitation in Insulating Crystals. *J. Chem. Phys.* **1958**, *28*, 647–650.
- (2) Kenkre, V. M.; Reineker, P. *Exciton Dynamics in Molecular Crystals and Aggregates*; Springer-Verlag: Berlin; New York, 1982.
- (3) Silinsh, E.; Capek, V. *Exciton Dynamics in Molecular Crystals and Aggregates*; American Institute of Physics: New York, 1994.
- (4) May, V.; Kühn, O. *Charge and Energy Transfer Dynamics in Molecular Systems*; Wiley-VCH: Weinheim, 2011.
- (5) Dimitriev, O. P. Dynamics of Excitons in Conjugated Molecules and Organic Semiconductor Systems. *Chem. Rev.* **2022**, *122*, 8487–8593.
- (6) Barford, W. Exciton dynamics in conjugated polymer systems. *Front. Phys.* **2022**, *10*, No. 1004042.
- (7) Haken, H.; Strobl, G. Exactly Solvable Model for Coherent and Incoherent Exciton Motion. *Z. Phys. A: Hadrons Nucl.* **1973**, *262*, 135–148.
- (8) Rebertrost, P.; Mohseni, M.; Kassal, I.; Lloyd, S.; Aspuru-Guzik, A. Environment-assisted quantum transport. *New J. Phys.* **2009**, *11*, No. 033003.
- (9) Kunsel, T.; Jansen, T. L. C.; Knoester, J. Scaling relations of exciton diffusion in linear aggregates with static and dynamic disorder. *J. Chem. Phys.* **2021**, *155*, No. 134305.
- (10) Schwarzer, E.; Haken, H. Moments of Coupled Coherent and Incoherent Motion of Excitons. *Phys. Lett. A* **1972**, *A 42*, 317–318.
- (11) Tutunnikov, I.; Chuang, C. R.; Cao, J. S. Coherent Spatial Control of Wave Packet Dynamics on Quantum Lattices. *J. Phys. Chem. Lett.* **2023**, *14*, 11632–11639.
- (12) Equation 22 was confirmed by numerical solutions of the stochastic TDSE.
- (13) Fratini, S.; Mayou, D.; Ciuchi, S. The Transient Localization Scenario for Charge Transport in Crystalline Organic Materials. *Adv. Funct. Mater.* **2016**, *26*, 2292–2315.
- (14) Chuang, C.; Lee, C. K.; Moix, J. M.; Knoester, J.; Cao, J. S. Quantum Diffusion on Molecular Tubes: Universal Scaling of the 1D to 2D Transition. *Phys. Rev. Lett.* **2016**, *116*, No. 196803.
- (15) Nitzan, A. *Chemical Dynamics in Condensed Phases: Relaxation, Transfer and Reactions in Condensed Molecular Systems*; Oxford University Press: Oxford; New York, 2006.
- (16) Breuer, H.-P.; Petruccione, F. *The Theory of Open Quantum Systems*; Oxford University Press: Oxford, New York, 2002.
- (17) Zhong, X. X.; Zhao, Y. Non-Markovian stochastic Schrödinger equation at finite temperatures for charge carrier dynamics in organic crystals. *J. Chem. Phys.* **2013**, *138*, No. 014111.
- (18) Han, L.; Ke, Y. L.; Zhong, X. X.; Zhao, Y. Time-Dependent Wavepacket Diffusion Method and its Applications in Organic Semiconductors. *Int. J. Quantum Chem.* **2015**, *115*, 578–588.
- (19) Suess, D.; Strunz, W. T.; Eisfeld, A. Hierarchical Equations for Open System Dynamics in Fermionic and Bosonic Environments. *J. Stat. Phys.* **2015**, *159*, 1408–1423.
- (20) Hsieh, C. Y.; Cao, J. S. A unified stochastic formulation of dissipative quantum dynamics. I. Generalized hierarchical equations. *J. Chem. Phys.* **2018**, *148*, No. 014103.
- (21) Mannouch, J. R.; Richardson, J. O. A mapping approach to surface hopping. *J. Chem. Phys.* **2023**, *158*, No. 104111.
- (22) Runeson, J. E.; Manolopoulos, D. E. A multi-state mapping approach to surface hopping. *J. Chem. Phys.* **2023**, *159*, No. 094115.
- (23) Moix, J. M.; Khasin, M.; Cao, J. S. Coherent quantum transport in disordered systems: I. The influence of dephasing on the transport properties and absorption spectra on one-dimensional systems. *New J. Phys.* **2013**, *15*, 085010.

(24) Tannor, D. J. *Introduction to Quantum Mechanics: A Time-Dependent Perspective*; University Science Books: Sausalito, California, 2007.

(25) Likewise, the quantum to classical transition for an initial Gaussian wave function may be inferred by time-integrating the diffusion coefficient for the Gaussian initial state, as shown in [Figure 1](#), to obtain $\text{MSD}(t)$.

(26) Daley, A. J. Quantum trajectories and open many-body quantum systems. *Adv. Phys.* **2014**, *63*, 77–149.